

# A dynamical model of surrogate reactions

Y. Aritomo, S. Chiba and K. Nishio

*Advanced Science Research Center,*

*Japan Atomic Energy Agency, Tokai, Ibaraki, 319-1195, Japan*

## Abstract

A new dynamical model is developed to describe the whole process of surrogate reactions; transfer of several nucleons at an initial stage, thermal equilibration of residues leading to washing out of shell effects and decay of populated compound nuclei are treated in a unified framework. Multi-dimensional Langevin equations are employed to describe time-evolution of collective coordinates with a time-dependent potential energy surface corresponding to different stages of surrogate reactions. The new model is capable of calculating spin distributions of the compound nuclei, one of the most important quantity in the surrogate technique. Furthermore, various observables of surrogate reactions can be calculated, e.g., energy and angular distribution of ejectile, and mass distributions of fission fragments. These features are important to assess validity of the proposed model itself, to understand mechanisms of the surrogate reactions and to determine unknown parameters of the model. It is found that spin distributions of compound nuclei produced in  $^{18}\text{O}+^{238}\text{U} \rightarrow ^{16}\text{O}+^{240*}\text{U}$  and  $^{18}\text{O}+^{236}\text{U} \rightarrow ^{16}\text{O}+^{238*}\text{U}$  reactions are equivalent and much less than  $10\hbar$ , therefore satisfy conditions proposed by Chiba and Iwamoto (PRC 81, 044604(2010)) if they are used as a pair in the surrogate ratio method.

PACS numbers: 24.87.+y, 24.10.-i, 24.60.Ky, 27.90.+b

## I. INTRODUCTION

Neutron-induced cross section data of unstable nuclei are systematically required to design next-generation nuclear facilities such as high burn-up fast breeder reactors or accelerator-driven systems for transmutation of nuclear wastes [1]. Such data are also important to understand origin of elements, namely, the s- and r-process nucleosynthesis (see, e.g., Refs. [2, 3]). However, it is not usually possible to measure these cross sections directly by using neutrons due to difficulty in preparing samples. It is well known that the compound reaction process is the dominant mechanism in the energy region of our interest. Therefore, various experimental methods to measure the “direct” neutron capture components are not applicable to determine them. Instead, other methods are needed, and one of the promising method is the surrogate reaction approach [4–25]. In this method, (multi) nucleon transfer reactions with an experimentally accessible combination of projectile and target are employed to create the same compound nucleus as the desired neutron reaction, and decay branching ratios to specific channels, normally capture and/or fission, are determined. However, branching ratios are sensitive to the spin and parity of the compound state, while the spin-parity ( $J^\pi$ ) distributions of populated nuclei are probably different for the neutron-induced and surrogate reactions. It is well known that if the spin is different even just 1 unit, the capture branching ratio is totally different for the energy region of our interest. Therefore, validity of the surrogate method depends on how the difference of the spin-parity distributions is comprehended and compensated properly.

Recently, the surrogate ratio method (SRM) is discussed by Chiba and Iwamoto. It was found that SRM works to a certain accuracy if (1) there exist two surrogate reactions whose spin-parity distributions of decaying nuclei are equivalent, (2) difference of representative spin values between the neutron-induced and surrogate reactions is not much larger than  $10 \hbar$ , under a condition that (3) weak Weisskopf-Ewing condition, namely,  $J^\pi$ -by- $J^\pi$  convergence of the branching ratio, is realized [26]. They form a set of sufficient conditions for the SRM to work. It is important to notice that the  $J^\pi$  distribution may be even different for the neutron-induced and surrogate reactions if these conditions are fulfilled.

Discovery of the above conditions is a great advancement for the whole surrogate technique. Therefore we need further investigation to verify that the above conditions, especially (1) and (2) which were just assumed in Ref. [26], are really satisfied in certain surrogate

reactions. It implies that mechanisms of the surrogate reactions to be understood well. For that aim, it is indispensable to establish a theoretical model to describe the whole process of the surrogate reactions, namely, nucleon transfer and decay of populated compound nucleus.

In this work, we propose a first version of our model to describe the surrogate reactions based on a theory proposed originally by Zagrebaev and Greiner [27]. This model, called a unified model, can treat the whole reaction processes in heavy- and superheavy-mass regions, which has been applied to several types of reactions [27–30]. The name of unified model implies an unified dynamical approach and unified multidimensional potential energy. Time-evolution of the system is described by a trajectory calculation on the time-dependent unified potential energy surface using the Langevin equation. Then, we treat a two neutron transfer reaction;  $^{18}\text{O}+^{238}\text{U} \rightarrow ^{16}\text{O}+^{240}\text{U}$ , which is planned to be employed at Japan Atomic Energy Agency (JAEA) as an example of application of the new model to the surrogate reaction. By using the new model, we can obtain various quantities which can be compared with experimental data directly and we can evaluate our theory and determine unknown parameters in the model.

The purpose of this paper is to explain the new model, calculate a fission fragment mass distribution (FFMD) for a reaction  $^{18}\text{O}+^{238}\text{U}$  to calibrate the model parameter, and calculate spin distributions of compound nuclei for the  $^{18}\text{O}+^A\text{U} \rightarrow ^{16}\text{O}+^{A+2*}\text{U}$  system, where  $A=236$  and  $238$ , to see if the conditions proposed by Chiba and Iwamoto are satisfied or not. In section 2, we explain our theoretical framework. The calculation results are presented in section 3. In section 4, we present a summary of this study and further discussion.

## II. DYNAMICAL MODEL

### A. Overview of the model

The surrogate reactions consist of 2 stages; an initial nucleon transfer process and decay of populated compound nuclei, which have quite different nature to each other. The Hauser-Freshbach (HF) theory [31, 32] has been applied to describe the latter part of the surrogate reactions. By the HF theory, we are able to calculate decay branching ratios to specific channels (capture or fission) with arbitrary spin-parity distributions of compound states. However, we cannot predict the spin distribution produced by the initial stage of the

surrogate reaction nor the FFMD with the HF theory. For that reason, we need to describe the whole reaction process consistently, i.e., starting from the transfer of several nucleons and the decay of the compound nucleus leading to fission successively. Here, we employ a dynamical model, the unified model, to the surrogate reaction.

The unified model was proposed by Zagrebaev and Greiner and was applied to several types of reactions [27–30] induced by heavy ions. An unified dynamical approach and unified multidimensional potential energy are employed in this model, which are the origin of the name of this theory. To apply this model to the surrogate reaction, we extend this model and introduce new procedures. As explained above, the surrogate reactions consist of two processes; the transfer reaction process between a two-body system and decay of the populated compound nuclei (one-body system), for which the mass of total system is different very much to each other. Therefore, it is indispensable to connect such different systems to treat surrogate reactions consistently. Evolution of the mass-asymmetry parameter is described by multi-dimensional Langevin equations without (with) the inertia parameter before (after) the window of the colliding nuclei opens sufficiently. We modify the original unified model [27] also to take account of temperature dependence of the shell correction energy of the potential energy surface.

Firstly, we treat the transfer reaction process within the framework of the unified model. Then, we treat the decay of the compound nuclei with an initial condition populated by the former reaction process. We perform a trajectory calculation on a time-dependent potential energy surface corresponding to different stages of the surrogate reaction. A dynamical calculation is carried out in terms of the multi-dimensional Langevin equation based on the fluctuation-dissipation theorem. By this procedure, we can describe trajectories moving on the potential energy surface including the nucleon transfer reaction.

We consider in this paper a two neutron transfer reaction  $^{18}\text{O}+^{238}\text{U} \rightarrow ^{16}\text{O}+^{240*}\text{U}$  as an example. In the transfer reaction process, we use the potential energy of  $^{256}\text{Fm}$  as the total system. After the production of the compound nucleus by the transfer reaction, we then treat the decay of the compound nucleus  $^{240}\text{U}$ . In other words, the potential energy surface switches from that of  $^{256}\text{Fm}$  to that of  $^{240}\text{U}$  as the surrogate reactions proceed from the transfer process to the decay stage.

A schematic picture of our model is presented in Fig. 1. It shows the potential energy surfaces used in the trajectory calculation from the transfer process to the decay of compound

nuclei in the reaction  $^{18}\text{O}+^{238}\text{U} \rightarrow ^{16}\text{O}+^{240}\text{U}$ . The transfer reaction process is presented in the upper left panel of Fig. 1 which shows a diabatic potential energy surface of  $^{256}\text{Fm}$  in the  $z$ - $\alpha$  ( $\delta = 0$ ) coordinate space. Meanings of these parameters and terms are explained in the next subsection. The thin arrows correspond to the entrance and the exit channels of two-neutron transfer process. In the calculation, it starts from an infinite distance between the projectile and target, where actually the distance of 30 fm is used. Then, the calculation stops when the trajectory reaches at the distance of 25 fm between the both fragments. We select the two nucleon transfer among the all events; we select events in which the mass asymmetry parameter  $\alpha$  changes from 0.859 corresponding to  $^{18}\text{O}+^{238}\text{U}$  to 0.875 corresponding to  $^{16}\text{O}+^{240}\text{U}$ .

Next, the decay process of compound nucleus is presented in the lower right panel of Fig. 1, which is a potential energy surface of  $^{240}\text{U}$  with  $\delta = 0.2$  ( $\beta_2 \sim 0.2$ ). The white lines denote mean fission paths. In the decay process, we start the trajectory calculation with the initial condition obtained in the transfer reaction process. As the initial condition, we use the deformation, momentum, angular momentum and excitation energy of the compound nucleus. The quantities which we can obtain with this calculation are the angular and energy distributions of ejectile, mass and total kinetic energy distributions of fission fragments and neutron multiplicities, and so on. Such quantities can be compared with experimental data directly, which allows us to determine unknown parameter in the model. In this work, we discuss a mass distribution of fission fragments and determine a value of one of the most uncertain parameter, the sliding friction (see below). In this way, we can evaluate and improve our model step-by-step by comparing model predictions with experimental data. More details of our model will be explained below.

## B. Potential energy surface

The initial stage of the surrogate reaction consists of 2 parts; 1) a fast diabatic part in which the reaction proceeds too fast for nucleons to reconfigure their single-particle states so the system goes through the ground-state configurations of the target and projectile, and 2) the system relaxes to the ground-state of the total composite system, which changes the potential energy surface to an adiabatic one. Therefore, we take into account time evolution of the potential energies from the diabatic one  $V_{diab}(q)$  to the adiabatic one  $V_{adiab}(q)$ , here

$q$  denotes a set of collective coordinates representing the nuclear deformation. The diabatic potential is calculated by a folding procedure with effective nucleon-nucleon interaction [27, 28, 33], which is shown in the upper left part of Fig. 1. We can see a “potential wall” in the overlap region of the colliding system, which corresponds to a hard-core representing incompressibility of nuclear matter. On the other hand, the adiabatic potential energy of the system is calculated using an extended two-center shell model [33]. We then connect the diabatic and adiabatic potentials with a time-dependent weighting function as follows;

$$\begin{aligned} V &= V_{diab}(q)f(t) + V_{adiab}(q)[1 - f(t)], \\ f(t) &= \exp\left(-\frac{t}{\tau}\right). \end{aligned} \quad (1)$$

Here,  $t$  is the time of interaction and  $f(t)$  is the weighting function with the relaxation time  $\tau$ . We use a relaxation time  $\tau = 10^{-21}$  sec, which was suggested in references [34]. It is empirically known that calculated results do not depend noticeably on the relaxation time.

As the coordinates to express nuclear deformation, we use the two-center parametrization [35, 36] and employ three parameters as follows:  $z_0$  (distance between centers of two potentials),  $\delta$  (deformation of fragments), and  $\alpha$  (mass asymmetry of the colliding nuclei);  $\alpha = (A_1 - A_2)/(A_1 + A_2)$ , where  $A_1$  and  $A_2$  denote the mass numbers of the target and the projectile, respectively [37]. Later on,  $A_1$  and  $A_2$  are used to denote mass numbers of two fission fragments. The parameter  $\delta$  is defined as  $\delta = 3(a - b)/(2a + b)$ , where  $a$  and  $b$  denote the half length of the axes of ellipse in the  $z_0$  and  $\rho$  direction, respectively as expressed in Fig. 1 in reference [35]. We assume that each fragment has the same deformations as a first step. Furthermore, we use scaling to save computation time and employ a coordinate  $z$  defined as  $z = z_0/(R_{CN}B)$ , where  $R_{CN}$  denotes the radius of the spherical compound nucleus. The parameter  $B$  is defined as  $B = (3 + \delta)/(3 - 2\delta)$ .

In the two-center parametrization, the neck parameter is denoted by  $\epsilon$  and is known to be different in the entrance and exit channels [33]. Therefore, we employ  $\epsilon = 1$  for the entrance channel and  $\epsilon = 0.35$  for the exit channel to describe a realistic nuclear shape. We introduce a time-dependent potential energy surface in terms of  $\epsilon$  using a relaxation time for  $\epsilon$  of  $\tau_\epsilon = 10^{-20}$  sec [38], as follows;

$$\begin{aligned} V_{adiab} &= V_{adiab}(q, \epsilon = 1)f_\epsilon(t) + V_{adiab}(q, \epsilon = 0.35)[1 - f_\epsilon(t)], \\ f_\epsilon(t) &= \exp\left(-\frac{t}{\tau_\epsilon}\right). \end{aligned} \quad (2)$$

### C. Dynamical equations

We then perform trajectory calculations on the time-dependent unified potential energy using the Langevin equation [27, 28, 37]

The nucleon transfer for slightly separated nuclei is important in surrogate reactions. Such intermediate nucleon exchange plays an important role in fusion process at incident energies near and below the Coulomb barrier as well. We treat the nucleon transfer using the procedure described in reference [27, 28];

$$\frac{d\alpha}{dt} = \frac{2}{A_{CN}} D_A^{(1)}(\alpha) + \frac{2}{A_{CN}} \sqrt{D_A^{(2)}(\alpha) \Gamma_\alpha(t)}, \quad (3)$$

This is a Langevin equation neglecting inertia mass for the mass asymmetry parameter. It expresses change of the asymmetry parameter  $\alpha$  due to drift (first term on the right hand side) and diffusion (second term on the r.h.s.) processes. It is obtained by a certain approximation starting from the Master equation for transition of different particle-hole states. Such Master equation giving discrete change of nucleon numbers is transformed to an equation for a continuous variable  $\alpha$  via Fokker-Planck equation to the Langevin equation shown above[27, 28].

After the window of the touching nuclei opens sufficiently (hereafter “the mono-nucleus state”), the treatment of the evolution of the mass-asymmetric parameter  $\alpha$  switches from eq. (3) to the Langevin equations with the procedure described in reference [37]. The

multidimensional Langevin equations [27, 30, 37] are now unified as

$$\begin{aligned}
\frac{dq_i}{dt} &= (m^{-1})_{ij} p_j, \\
\frac{dp_i}{dt} &= -\frac{\partial V}{\partial q_i} - \frac{1}{2} \frac{\partial}{\partial q_i} (m^{-1})_{jk} p_j p_k - \gamma_{ij} (m^{-1})_{jk} p_k \\
&\quad + g_{ij} R_j(t), \\
\frac{d\theta}{dt} &= \frac{\ell}{\mu_R R^2}, \\
\frac{d\varphi_1}{dt} &= \frac{L_1}{\mathfrak{S}_1}, \\
\frac{d\varphi_2}{dt} &= \frac{L_2}{\mathfrak{S}_2}, \\
\frac{d\ell}{dt} &= -\frac{\partial V}{\partial \theta} - \gamma_{tan} \left( \frac{\ell}{\mu_R R} - \frac{L_1}{\mathfrak{S}_1} a_1 - \frac{L_2}{\mathfrak{S}_2} a_2 \right) R \\
&\quad + R g_{tan} R_{tan}(t), \\
\frac{dL_1}{dt} &= -\frac{\partial V}{\partial \varphi_1} + \gamma_{tan} \left( \frac{\ell}{\mu_R R} - \frac{L_1}{\mathfrak{S}_1} a_1 - \frac{L_2}{\mathfrak{S}_2} a_2 \right) a_1 \\
&\quad - a_1 g_{tan} R_{tan}(t), \\
\frac{dL_2}{dt} &= -\frac{\partial V}{\partial \varphi_2} + \gamma_{tan} \left( \frac{\ell}{\mu_R R} - \frac{L_1}{\mathfrak{S}_1} a_1 - \frac{L_2}{\mathfrak{S}_2} a_2 \right) a_2 \\
&\quad - a_2 g_{tan} R_{tan}(t),
\end{aligned} \tag{4}$$

where a summation over repeated indices is assumed. The collective coordinates  $q_i$  stands for  $z$ ,  $\delta$  and  $\alpha$ . The symbol  $p_i$  denotes momentum conjugate to  $q_i$ , and  $V$  is the multi-dimensional potential energy. Definition of other parameters is given in Fig. 2: The symbols  $\theta$  and  $\ell$  are the relative orientation of nuclei and relative angular momentum, respectively, and  $\varphi_1$  and  $\varphi_2$  denote the angles of rotation of the nuclei in the reaction plane (their moments of inertia and angular momenta are  $\mathfrak{S}_{1,2}$  and  $L_{1,2}$ , respectively),  $a_{1,2} = R/2 \pm (R_1 - R_2)/2$  are the distances from the centers of the fragments up to the middle point between nuclear surfaces, and  $R_{1,2}$  are the nuclear radii. The symbol  $R$  is the distance between the nuclear centers. The total angular momentum  $L = \ell + L_1 + L_2$  is conserved. The symbol  $\mu_R$  denotes the reduced mass, and  $\gamma_{tan}$  is the friction force in the tangential direction of colliding nuclei, here we call it as the sliding friction.

The symbols  $m_{ij}$  and  $\gamma_{ij}$  stand for elements of the shape-dependent collective inertia and friction tensors, respectively. For separated nuclei, we use the reduced mass and the phenomenological friction forces with the Woods-Saxon radial form factor as described in reference [27, 28]. We switch the phenomenological friction to the friction for mono-nuclear



system using a smoothing function [27, 28]. For the mono-nuclear system, the wall-and-window one-body dissipation is adopted for the friction tensor, and a hydrodynamical inertia tensor is adopted in the Werner-Wheeler approximation for the velocity field [39–41]. The normalized random force  $R_i(t)$  is assumed to be of white noise, *i.e.*,  $\langle R_i(t) \rangle = 0$  and  $\langle R_i(t_1)R_j(t_2) \rangle = 2\delta_{ij}\delta(t_1 - t_2)$ . Strength of the random force  $g_{ij}$  is given by Einstein relation;  $\gamma_{ij}T = \sum_k g_{ij}g_{jk}$ , where  $T$  is the temperature of the compound nucleus calculated from the intrinsic energy of the composite system.

The adiabatic potential energy is defined as

$$V_{adiab}(q, L, T) = V_{LD}(q) + \frac{\hbar^2 L(L+1)}{2I(q)} + V_{SH}(q, T), \quad (5)$$

$$V_{LD}(q) = E_S(q) + E_C(q), \quad (6)$$

$$V_{SH}(q, T) = E_{shell}^0(q)\Phi(T), \quad (7)$$

$$\Phi(T) = \exp\left(-\frac{E^*}{E_d}\right), \quad (8)$$

where  $I(q)$  stands for the moment of inertia of a rigid body with deformation  $q$ ,  $V_{LD}$  and  $V_{SH}$  are the potential energy of the finite-range liquid drop model and the shell correction energy taking into account the temperature dependence, respectively. The symbol  $E_{shell}^0$  denotes the shell correction energy at  $T = 0$ . The temperature dependent factor  $\Phi(T)$  is discussed in reference [42], where  $E^*$  denotes the excitation energy of the compound nucleus. The shell damping energy  $E_d$  is chosen as 20 MeV, which is given by Ignatyuk et al. [43].

The symbols  $E_S$  and  $E_C$  denote a generalized surface energy [44] and Coulomb energy, respectively. The centrifugal energy arising from the angular momentum  $L$  of the rigid body is also considered. The intrinsic energy of the composite system  $E_{int}$  is calculated for each trajectory as

$$E_{int} = E^* - \frac{1}{2} (m^{-1})_{ij} p_i p_j - V(q, L, T). \quad (9)$$

Here,  $E^*$  is given by  $E^* = E_{cm} - Q$ , where  $Q$  and  $E_{cm}$  denote the  $Q$ -value of the reaction and the incident energy in the center-of-mass frame, respectively. Each trajectory starts from a sufficiently large distance between both nuclei [30].

#### D. Computation

Due to difference of the initial impact parameters (or the different initial relative angular momenta), various kind of reaction processes can occur. Moreover, even the trajectories start

with the same initial impact parameter, reactions proceed in quite different ways due to the random force in the dynamical equation, which finally leads to different reaction channels. By choosing various impact parameters randomly and give proper weights, whole processes of reactions are described by the present model; the elastic and inelastic scattering, deep inelastic collision, quasi-fission, fusion-fission process, and a few nucleon transfer process (the surrogate reaction). They are treated simultaneously by the model. This is a big advantage of the present approach, since these reactions correlate, thus they can give information to each other. An example is a determination of the unknown parameter  $\gamma_{tan}$  through FFMD of fusion-fission like process as will be discussed below.

### III. RESULTS AND DISCUSSION

The unified model, on which the present model is based, has been applied to several types of reactions and succeeded to describe the experimental data [27–30]. In our previous study, we precisely investigated the incident energy dependence of mass distribution of fission fragments in the reactions  $^{36}\text{S}+^{238}\text{U}$  and  $^{30}\text{Si}+^{238}\text{U}$  [30, 45, 46]. The calculation results reproduced the experimental data well and clarified the origin of the fine structure of the mass distribution of fission fragments at the low incident energy.

Here, we apply the present model to the surrogate reaction. To evaluate and clarify the model, we focus on the mass distribution of the fission fragments and compare calculated results with experimental data. Furthermore, we investigate spin distributions of the compound nucleus populated by transfer reactions and discuss the validity condition of the SRM[26]. We choose a system of  $^{18}\text{O}+^A\text{U} \rightarrow ^{16}\text{O}+^{A+2*}\text{U}$  reaction where  $A = 236$  or/and  $238$ .

In the Langevin calculation, the sliding friction is mainly responsible for the dissipation of the angular momentum [48, 49], though its value is uncertain. In the present work, we treat the sliding friction as a parameter of the model and investigate dependence of the calculation upon this parameter. Measured FFMD data in the reaction  $^{18}\text{O}+^{238}\text{U}$  at  $E_{c.m} = 133.5$  MeV is shown by dots in Fig. 3. It includes all the fission fragments occurring in the above reaction. The experimental set-up and the data analysis are nearly the same as the references [45, 47]. In the experiment, both fission fragments were detected in coincidence by using position-sensitive multiwire proportional counters (MWPCs). The difference of the setup from the references [45, 47] was the angles of the detector positions that MWPC1 and

MWPC2 were located at  $-90^\circ$  and  $+90^\circ$  with respect to the beam direction.

In Fig. 3, calculated data with  $\gamma_{tan} = 1, 5, 10$  and  $20 \times 10^{-22}$  MeV s fm $^{-2}$  are denoted by the black, red, green and dark blue histograms, respectively. It is clearly seen that the result with  $\gamma_{tan} = 5$  reproduces the experimental data very well. With larger sliding friction, the variance of results becomes smaller. We can fix values of unknown parameters in this way.

Then, calculations for the 2 neutron transfer reaction are carried out without any adjustable parameters. From such calculations, we can determine spin distributions of the surrogate reactions  $^{18}\text{O}+^{236}\text{U} \rightarrow ^{16}\text{O}+^{238*}\text{U}$  and  $^{18}\text{O}+^{238}\text{U} \rightarrow ^{16}\text{O}+^{240*}\text{U}$ , and verify if the 2 assumptions proposed by Chiba and Iwamoto[26], namely, (1) there exist two surrogate reactions whose spin-parity distributions of decaying nuclei are almost equivalent, and (2) difference of representative spin values between the neutron-induced and surrogate reactions is not much larger than  $10 \hbar$ , are really satisfied or not.

Figure 4 shows calculated spin distributions of compound nucleus  $^{240}\text{U}$  populated in the reaction  $^{18}\text{O}+^{238}\text{U} \rightarrow ^{16}\text{O}+^{240}\text{U}$  at an incident energy of  $E_{c.m.} = 160$  MeV, which is planned to be carried out at JAEA. Results with various values of the sliding friction are shown. We can see that majority of the spin of compound nucleus is much less than  $10 \hbar$  for each value of the sliding friction although they diverge depending on  $\gamma_{tan}$ . Therefore, it is important for the model to have a capability to determine values of unknown parameters as shown above. Our model is particularly powerful since this parameter is determined by using observables corresponding to other reaction channels, which can be treated simultaneously with the surrogate reactions of our interest. Figure 5 shows spin distributions of compound nuclei  $^{240}\text{U}$  and  $^{238}\text{U}$  in the transfer reactions  $^{18}\text{O}+^{238}\text{U} \rightarrow ^{16}\text{O}+^{240}\text{U}$  and  $^{18}\text{O}+^{236}\text{U} \rightarrow ^{16}\text{O}+^{238}\text{U}$ , respectively with the sliding friction  $\gamma_{tan} = 5 \times 10^{-22}$  [MeV s fm $^{-2}$ ]. These distributions should be interpreted as a semi-classical estimate of a spin distribution corresponding to excitation of rotational motion due to angular momentum transfer occurring in these reactions. It is easily noticed that the spin distributions of the compound nuclei populated by the two reactions are almost equivalent. These results suggest that the assumptions (1) and (2) shown above for the SRM to work[26] are proved to be correct within this model. In conjunction with the weak Weisskopf-Ewing condition proposed in Ref. [26] (which can be verified by Hauser-Feshbach theory), the present result suggests that  $^{18}\text{O}+^{238}\text{U} \rightarrow ^{16}\text{O}+^{240}\text{U}$  and  $^{18}\text{O}+^{236}\text{U} \rightarrow ^{16}\text{O}+^{238}\text{U}$  reactions can be employed as a pair in the SRM.

We propose that this model as a powerful and useful tool to describe the surrogate

reaction process, even though it is a semi-classical model. To describe the transfer reaction process more accurately, we may have to consider quantum effects precisely. Quantum mechanical models such as DWBA or CDCC [50] would be more appropriate to describe the nucleon-transfer part of the surrogate reactions. It will be absolutely necessary if we use light-ion projectiles. We can use these sophisticated models if they are available and connect the populated spin-distribution to the later part of the present model. However, it is difficult to treat transition probabilities to continuous levels quantum mechanically as realized in surrogate reactions. As the first step, therefore, we try to understand the gross feature of the surrogate reaction and analyze the reaction mechanism using the present model in this paper. Especially, it is known that the dynamical model is useful to discuss the mass distribution of fission fragments [51, 52], an important observable of the surrogate reactions which contains information on the populated compound nuclei such as the spin distribution[53].

#### IV. SUMMARY

We propose a first version of a unified dynamical theory to describe the whole process of surrogate reactions; the nucleon transfer, thermalization and the decay of the populated compound nuclei. To realize it, we introduced new procedures to the unified theory of Zagrebaev and Greiner, namely, switching of the potential energy surfaces having very different mass numbers, Langevin equations depending on different stages of the reaction and a temperature-dependent shell correction energy. Trajectory calculations in terms of the Langevin equations are employed on a time-dependent potential energy surface corresponding to different stages of the surrogate reactions. After the transfer process, decay of the populated compound nucleus is calculated with the initial condition obtained from the preceding transfer process. This model can yield many observables which can be compared with experimental data directly.

As an example of the application of the present model to surrogate reactions, we considered a two nucleon transfer reaction;  $^{18}\text{O}+^{238}\text{U} \rightarrow ^{16}\text{O}+^{240}\text{U}$ , which is planned to be performed at JAEA. We treated the sliding friction as a parameter of the model and discussed the dependence of the calculation results upon the sliding friction. Then, we discussed the validity condition of the surrogate ratio method (SRM). We calculated the spin distribution

of the compound nuclei with several sliding frictions for the compound nucleus  $^{240}\text{U}$  in the reaction  $^{18}\text{O}+^{238}\text{U} \rightarrow ^{16}\text{O}+^{240}\text{U}$  at the incident energy of  $E_{c.m.} = 160$  MeV. The calculation results showed that the spin of compound nucleus was less than  $10\hbar$  for each value of the sliding friction. Finally, we discussed spin distributions of compound nucleus  $^{240}\text{U}$  and  $^{238}\text{U}$  in the transfer reactions  $^{18}\text{O}+^{238}\text{U} \rightarrow ^{16}\text{O}+^{240}\text{U}$  and  $^{18}\text{O}+^{236}\text{U} \rightarrow ^{16}\text{O}+^{238}\text{U}$ , respectively. It was found that the spin distributions of decaying nuclei populated by the two reactions are almost equivalent. Therefore it is concluded that if these reactions are used as a pair in the SRM, they would yield the correct neutron cross sections[26]. These calculation results suggested validity of the SRM within this model.

In the present model, however, nuclei were treated as nuclear matter, and a semi-classical approach was employed except for the fact that we took into account the shell correction energy on the potential energy surface. Such semi-classical model may be too simple, and we may have to consider quantum effects in order to describe the reactions more accurately. Nevertheless, the present model is flexible enough to take account of results of more elaborated models. We therefore consider that the present model is capable enough, as a first step, to understand gross features of the surrogate reactions which itself is already quite complicated.

As further studies, we improve the model in the nucleon transfer part by taking into account the quantum effect more precisely. After experiments of the surrogate reaction at JAEA are performed, we can compare model predictions with experimental data, e.g., distributions of emission angle and energy loss of ejectile, mass, charge and total kinetic energy distributions of fission fragments from various exclusive fission channels, and the model will be upgraded successively.

## V. ACKNOWLEDGMENTS

The authors are grateful to Prof. V.I. Zagrevaev for helpful suggestions and valuable discussion. The special thanks are deserved to Dr. S. Hashimoto for his helpful comments. The diabatic potential and adiabatic potential were calculated using the NRV code [33]. A part of the numerical calculations was carried out on SX8 at YITP in Kyoto University. Present study is the result of "Development of a Novel Technique for Measurement of Nuclear Data Influencing the Design of Advanced Fast Reactors" entrusted to Japan Atomic Energy

Agency (JAEA) by the Ministry of Education, Culture, Sports, Science and Technology of Japan (MEXT).

- 
- [1] International Atomic Energy Agency (Editor), *Fission Product Yield Data for the Transmutation of Minor Actinide Nuclear Waste* (IAEA, Vienna, 2008).
- [2] D. Arnett, " *Supernovae and Nucleosynthesis*", Princeton University Press (1996).
- [3] B.E.J. Pagel, " *Nucleosynthesis and Chemical Evolution of Galaxies*", Cambridge University Press (1997).
- [4] J.D. Cramer and H.C. Britt, Phys. Rev. C **2**, 2350 (1970).
- [5] J.D. Cramer and H.C. Britt, Nucl. Sci. Eng. **41**, 177 (1970).
- [6] B.B. Back, O. Hansen, H.C. Britt, and J.D. Garrett, Phys. Rev. C **9**, 1924 (1974).
- [7] B.B. Back, H.C. Britt, O. Hansen, B. Leroux, and J.D. Garrett, Phys. Rev. C **10**, 1948 (1974).
- [8] H.C. Britt and J.B. Wilhelmy, Nucl. Sci. Eng. **72**, 222 (1979).
- [9] W. Younes and H.C. Britt, Phys. Rev. C **67**, 024610 (2003).
- [10] W. Younes and H.C. Britt, Phys. Rev. C **68**, 034610 (2003).
- [11] M. Petit *et al.*, Nucl. Phys. A **735**, 347 (2004).
- [12] C. Plettner *et al.*, Phys. Rev. C **71**, 051602(R) (2005).
- [13] S. Boyer *et al.*, Nucl. Phys. A **775**, 175 (2006).
- [14] J.T. Burke *et al.*, Phys. Rev. C **73**, 054604 (2006).
- [15] J.E. Escher and F.S. Dietrich, Phys. Rev. C **74**, 054601 (2006).
- [16] B.F. Lyles, L.A. Bernstein, J.T. Burke, F.S. Dietrich, J. Escher, I.J. Thompson, D.L. Bleuel, R.M. Clark, P. Fallon, J. Gibelin, A.O. Macchiavelli, M.A. McMahan, L. Phair, E. Rodriguez-Vieitez, M. Wiedeking, C.W. Beausang, S.R. Leshner, B. Darakchieva and M. Evtimova, Phys. Rev. C **76**, 014606 (2007).
- [17] C. Forssén, F.S. Dietrich, J. Escher, R.D. Hoffman and K. Kelley, Phys. Rev. C **75**, 055807 (2007).
- [18] B. Jurado, G. Kessedjian, M. Aiche *et al.*, AIP Conf. Proc. **1005**, 90 (2008).
- [19] S.R. Leshner, J.T. Burke, L.A. Bernstein, H. Ai, C.W. Beausang, D.L. Bleuel, R.M. Clark, F.S. Dietrich, J.E. Escher, P. Fallon, J. Gibelin, B.L. Goldblum, I.Y. Lee, A.O. Macchiavelli, M.A. McMahan, K.J. Moody, E.B. Norman, L. Phair, E. Rodriguez-Vieitez, N.D. Scielzo and M. Wiedeking, Phys. Rev. C **79**, 044609 (2009).

- [20] J.M. Allmond, L.A. Bernstein, C.W. Beausang, L. Phair, D.L. Bleuel, J.T. Burke, J.E. Escher, K.E. Evans, B.L. Goldblum, R. Hatarik, H.B. Jeppesen, S.R. Leshner, M.A. McMahan, J.O. Rasmussen, N.D. Scielzo and M. Wiedeking, Phys. Rev. C **79**, 054610 (2009).
- [21] R. Hatarik, L.A. Bernstein, J.A. Cizewski, D.L. Bleuel, J.T. Burke, J.E. Escher, J. Gibelin, B.L. Goldblum, A.M. Hatarik, S.R. Leshner, P.D. O'Malley, L. Phair, E. Rodriguez-Vieitez, T. Swan and M. Wiedeking, Phys. Rev. C **81**, 011602(R) (2010).
- [22] B.L. Goldblum, S.G. Prussin, L.A. Bernstein, W. Younes, M. Guttormsen and H.T. Nyhus, Phys. Rev. C **81**, 054606(2010).
- [23] J.E. Escher and F.S. Dietrich, Phys. Rev. C **81**, 024612(2010).
- [24] N.D. Scielzo, J.E. Escher, J.M. Allmond, M.S. Basunia, C.W. Beausang, L.A. Bernstein, D.L. Bleuel, J.T. Burke, R.M. Clark, F.S. Dietrich, P. Fallon, J. Gibelin, B.L. Goldblum, S.R. Leshner, M.A. McMahan, E.B. Norman, L. Phair, E. Rodriguez-Vieitez, S.A. Sheets, I.J. Thompson and M. Wiedeking, Phys. Rev. C **81**, 034608(2010).
- [25] G. Kessedjian, B. Jurado, M. Aiche, G. Barreau, A. Budaud, S. Czajkowski, D. Dassié, B. Haas, L. Mathieu, L. Audouin, N. Capellan, L. Tassan-Got, J.N. Wilson, E. Berthoumieux, F. Gunsing, Ch. theisin, O. Serot, E. Bauge, I. Ahmad, J.P. Greene and R.V.F. Janssens, Phys. Lett. **B 692**, 297(2010).
- [26] S. Chiba and O. Iwamoto, Phys. Rev. C **81** (2010) 044604.
- [27] V. Zagrebaev and W. Greiner, J. Phys. G **31**, 825 (2005).
- [28] V. Zagrebaev and W. Greiner, J. Phys. G **34**, 1 (2007); V. Zagrebaev and W. Greiner, J. Phys. G **34**, 2265 (2007).
- [29] V. Zagrebaev and W. Greiner, Phys. Rev. Lett. **101**, 122701 (2008); V. Zagrebaev and W. Greiner, Phys. Rev. C **78**, 034610 (2008); V. Zagrebaev and W. Greiner, J. Phys. G **35**, 125103 (2008).
- [30] Y. Aritomo, Phys. Rev. C **80** (2009) 064604.
- [31] W. Hauser and H. Feshbach, Phys. Rev. **87**, 366 (1952).
- [32] P. Fröbrich and R. Lipperheide, *Theory of Nuclear Reactions* (Clarendon Press, Oxford, 1996).
- [33] V.I. Zagrebaev, A.V. Karpov, Y. Aritomo, M.A. Naumenko, and W. Greiner, Physics of Particles and Nuclei **38**, 469 (2007); NRV codes for driving potential, <http://nrv.jinr.ru/nrv/>.
- [34] G.F. Bertsch, Z. Phys. A **289**, 103 (1978); W. Cassing and W. Nörenberg, Z. Phys. A **401**, 467 (1983); A. Diaz-Torres, Phys. Rev. C **69**, 021603 (2004).



- [35] J. Maruhn and W. Greiner, *Z. Phys. A* **251**, 431 (1972).
- [36] K. Sato, A. Iwamoto, K. Harada, S. Yamaji, and S. Yoshida, *Z. Phys. A* **288**, 383 (1978).
- [37] Y. Aritomo and M. Ohta, *Nucl. Phys. A* **744**, 3 (2004).
- [38] A. Karpov, private communication.
- [39] J. Blocki, Y. Boneh, J.R. Nix, J. Randrup, M. Robel, A.J. Sierk, and W.J. Swiatecki, *Ann. Phys.* **113**, 330 (1978).
- [40] J.R. Nix and A.J. Sierk, *Nucl. Phys. A* **428**, 161c (1984).
- [41] H. Feldmeier, *Rep. Prog. Phys.* **50**, 915 (1987).
- [42] Y. Aritomo, *Nucl. Phys. A* **780**, 222 (2006).
- [43] A.N. Ignatyuk, G.N. Smirenkin, and A.S. Tishin, *Sov. J. Nucl. Phys.* **21**, 255 (1975).
- [44] H.J. Krappe, J.R. Nix, and A.J. Sierk, *Phys. Rev. C* **20**, 992 (1979).
- [45] K. Nishio, H. Ikezoe, S. Mitsuoka, I. Nishinaka, Y. Nagame, Y. Watanabe, T. Ohtsuki, K. Hirose, and S. Hofmann, *Phys. Rev. C* **77**, 064607 (2008).
- [46] K. Nishio, H. Ikezoe, I. Nishinaka, S. Mitsuoka, K. Hirose, T. Ohtsuki, Y. Watanabe, Y. Aritomo, S. Hofmann, *Phys. Rev. C* in press.
- [47] K. Nishio *et al.*, *Phys. Rev. C* **82**, 024611 (2010)
- [48] R. Bass, *Nuclear Reactions with Heavy Ions* (Berlin, Springer) p.265 (1980).
- [49] W.U. Schröder and J.R. Huizenga, Damped nuclear Reactions, *Treatise on Heavy-Ion Science* vol 2, edited by D.A. Bromley (New York, Plenum) p.140 (1984).
- [50] M. Kamimura, M. Yahiro, Y. Iseri, Y. Sakuragi, H. Kameyama, M. Kawai, *Prog. Theor. Phys. Suppl.* **89** 1 (1986).
- [51] A.V. Karpov, P.N. Nadtochy, D.V. Vanin, and G.D. Adeev, *Phys. Rev. C* **63**, 054610 (2001).
- [52] T. Asano, T. Wada, M. Ohta, and T. Ichikawa, *Prog. Theor. Phys, Supplement* **154** 457 (2004).
- [53] Y. Aritomo, S. Chiba and K. Nishio, to be submitted.

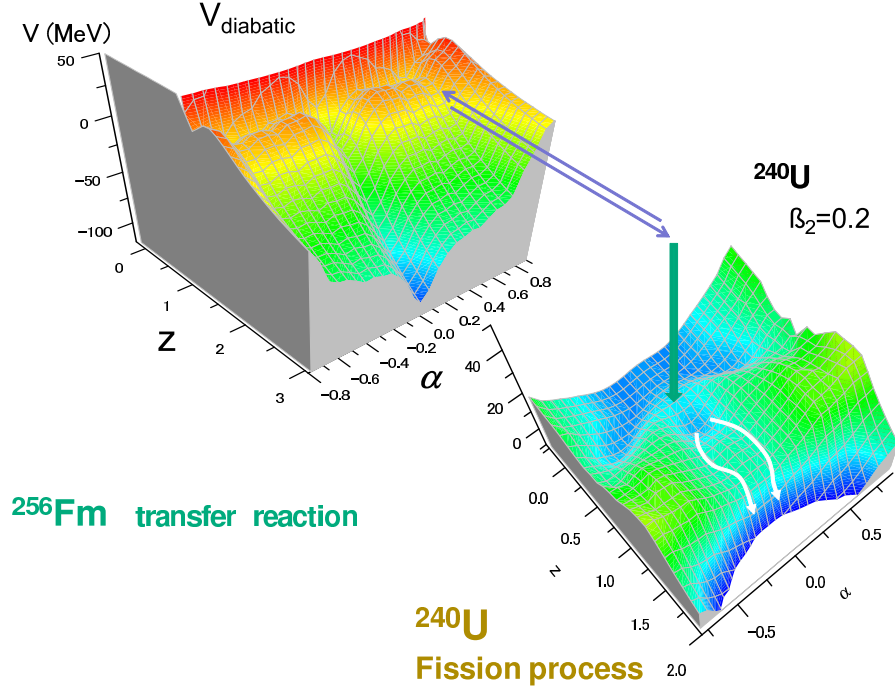


FIG. 1. (Color online) Schematic picture of the calculation. For the surrogate reaction  $^{18}\text{O}+^{238}\text{U} \rightarrow ^{16}\text{O}+^{240}\text{U}$ , the potential energy surfaces from the transfer reaction to the decay process of compound nuclei are presented. The transfer reaction is shown in the left panel which is the diabatic potential energy surface of  $^{256}\text{Fm}$  in the  $z - \alpha(\delta = 0)$  coordinate space. The decay process of compound nucleus is presented in the right panel, which is the adiabatic potential energy surface of  $^{240}\text{U}$  with  $\delta = 0.2$  ( $\beta_2 \sim 0.2$ ).

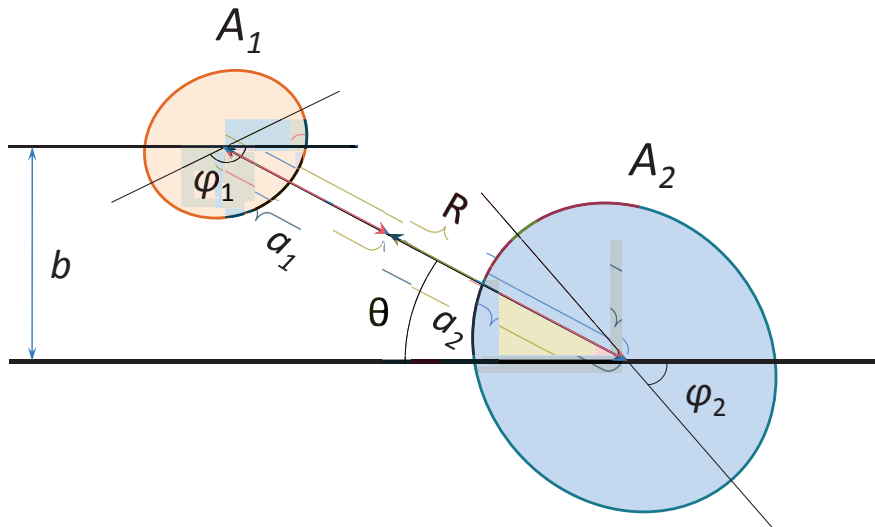


FIG. 2. (Color online) Definition of parameters used in the model.

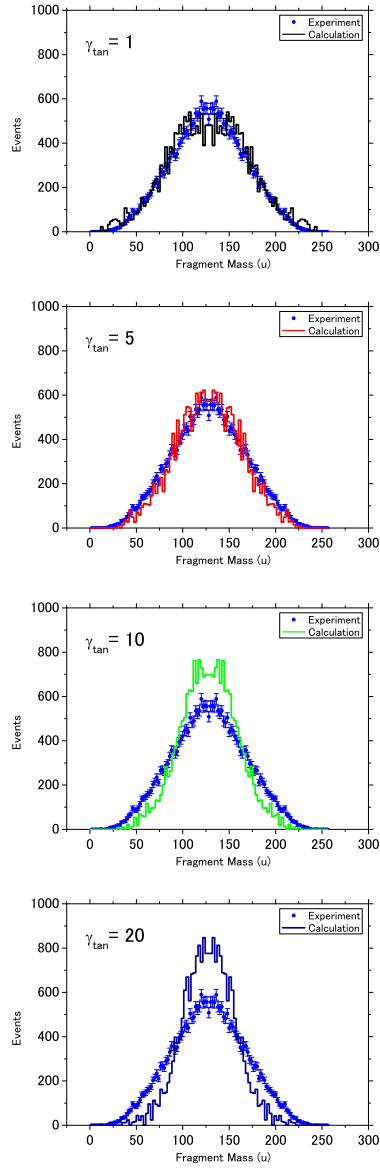


FIG. 3. (Color online) Fragment mass distribution obtained in the reaction  $^{18}\text{O}+^{238}\text{U}$  at an incident energy of  $E_{c.m.} = 133.5$  MeV. Experimental data and calculation results are denoted by circles and histograms, respectively. Calculations are shown with sliding frictions  $\gamma_{tan} = 1, 5, 10$  and  $20 \times 10^{-22}$  [MeV s fm $^{-2}$ ], which are multiplied by the factor such that the total cross section agree with the experimental value to compare the shape of the mass distribution with the experiment.

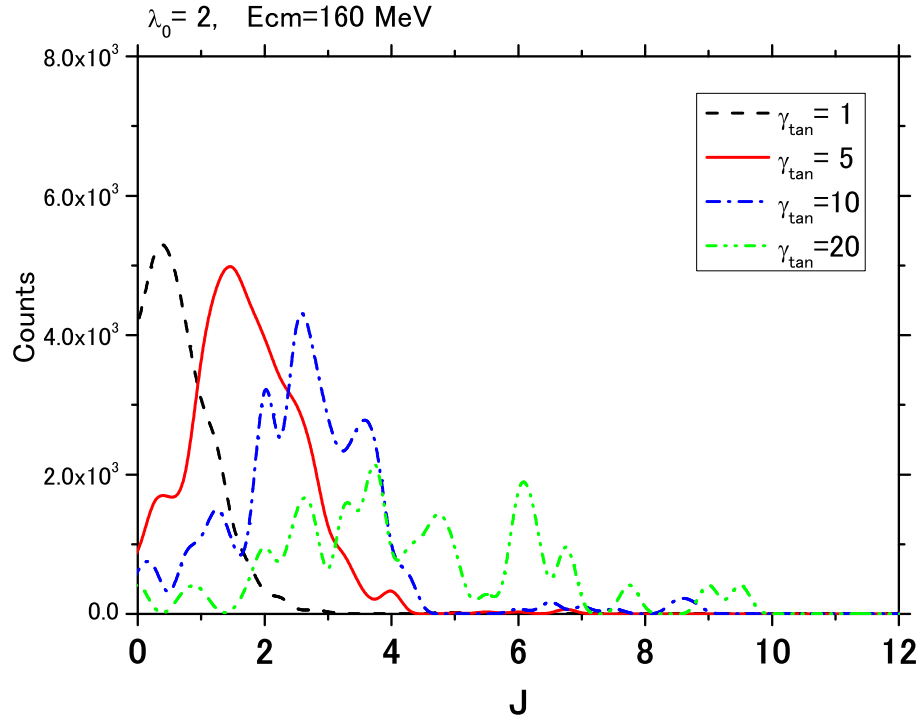


FIG. 4. (Color online) Spin distribution of compound nucleus  $^{240}\text{U}$  in the reaction  $^{18}\text{O}+^{238}\text{U} \rightarrow ^{16}\text{O}+^{240}\text{U}$  at the incident energy of  $E_{c.m.} = 160$  MeV for several sliding frictions. The black, red, blue and green lines denote for  $\gamma_{tan} = 1, 5, 10$  and  $20 \times 10^{-22}$  [MeV s fm $^{-2}$ ], respectively..

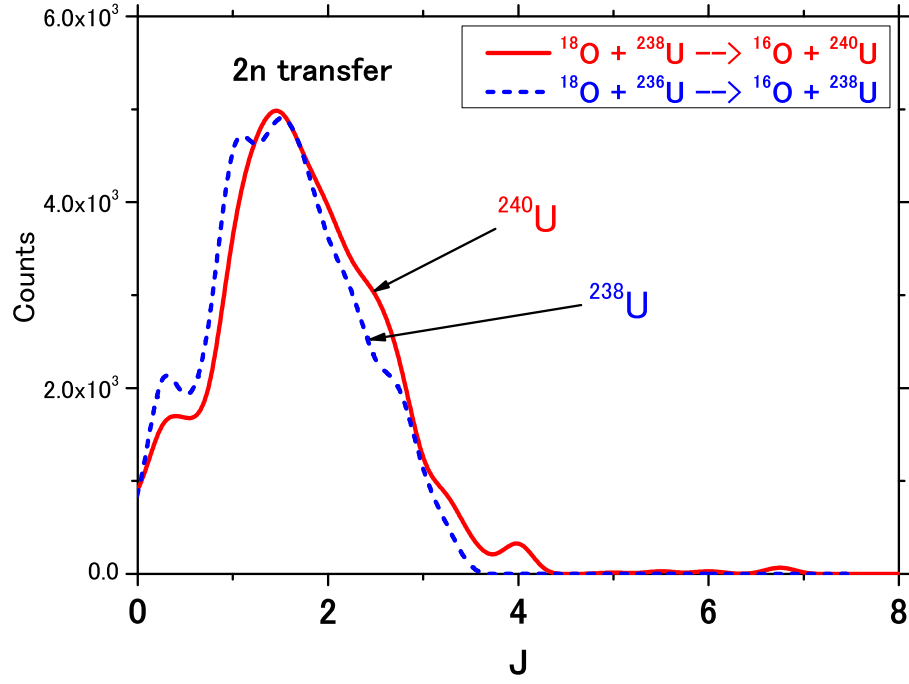


FIG. 5. (Color online) Spin distribution of compound nuclei  $^{240}\text{U}$  and  $^{238}\text{U}$  in the transfer reactions  $^{18}\text{O}+^{238}\text{U} \rightarrow ^{16}\text{O}+^{240}\text{U}$  and  $^{18}\text{O}+^{236}\text{U} \rightarrow ^{16}\text{O}+^{238}\text{U}$ , at the incident energy of  $E_{c.m.} = 160$  MeV, respectively. Sliding friction  $\gamma_{tan} = 5 \times 10^{-22}$  [MeV s fm $^{-2}$ ] is used.